A Hierarchical Self-Assembly Route to Three-Dimensional Polymer−Quantum Dot Photonic Arrays

Huda Yusuf, Whan-Gi Kim,† Dong Hoon Lee,† Marie Aloshyna, Alexandre G. Brolo, and Matthew G. Moffitt*

Department of Chemistry, University of Victoria, P.O. Box 3065, Victoria, British Columbia V8W 3V6, Canada, and Department of Applied Chemistry, Konkuk University, 322 Danwol, Chungju, Chungbuk, Korea 380-220

Received February 1, 2007. In Final Form: March 19, 2007

We demonstrate a new hierarchical self-assembly strategy for the formation of photonic arrays containing quantum dots (QDs), in which sequential self-assembly steps introduce organization on progressively longer length scales, ranging from the nanoscale to the microscale regimes. The first step in this approach is the self-assembly of diblock copolymers to form block ionomer reverse micelles (SA1); within each micelle core, a single CdS QD is synthesized to yield the hybrid building block BC−QD. Once SA1 is completed, the hydrophobic BD−QD building blocks are blended with amphiphilic block copolymer stabilizing chains in an organic solvent; water addition induces secondary self-assembly (SA2) to form quantum dot compound micelles (QDCMs). Finally, aqueous dispersions of QDCMs are slowly evaporated to induce the formation of three-dimensional (3D) close-packed arrays in a tertiary self-assembly step (SA3). The resulting hierarchical assemblies, consisting of a periodic array of hybrid spheres each containing multiple CdS QDs, exhibit the collective property of a photonic stop band, along with photoluminescence arising from the constituent QDs. A high degree of structural control is possible at each level of organization by judicious selection of experimental variables, allowing various parameters governing the collective optical properties, including QD size, nanoparticle spacing, and mesocale periodicity, to be independently tuned. The resulting control over optical properties via successive self-assembly steps should provide new opportunities for hierarchical materials for QD lasers and all-optical switching.

The controlled organization of colloidal semiconductor nanoparticles, or quantum dots (QDs), in three dimensions (3D) is essential to the production of devices and materials based on QDs. The collective properties of QD assemblies depend not only on the size and nature of the individual nanoparticle components but also on the interparticle spacing and ordering on multiple length scales. In recent years, there has been a particular interest in structures consisting of QDs distributed within photonic crystals,[1−12] which are materials with periodicity in the dielectric constant on the order of optical wavelengths. Bragg diffraction of light within photonic crystals gives rise to a stop band, or pseudogap, in which the propagation of light at specific wavelengths and in specific directions is prohibited.[13−18] For QDs embedded in a photonic crystal, light emission in the spectral region of the stop band can be either suppressed[2,3,11,12] or enhanced[1,3,11] according to Fermi's golden rule for the local density of electromagnetic states, opening up new possibilities for low-threshold microlasers and all-optical signal processing. Here, we present a new hierarchical self-assembly strategy for the formation of 3D photonic arrays containing QDs. The concept of hierarchical self-assembly, demonstrated previously by Whitesides using millimeter-scale beads,[19] involves a sequential series of different self-assembly steps in which the structures formed in each step are "frozen" and then used as building blocks (self-assembling elements) for the subsequent steps.

Several different routes have been previously demonstrated for the incorporation of QDs into photonic crystals.[1−12] QDs have been infused[5,11,12] and electrochemically[10] deposited within the voids of preassembled arrays of polymer or silica spheres. Alternatively, QDs have been incorporated into mesoscale spheres by layer-by-layer assembly[7,9] or by in situ synthesis[6,8] followed by the self-assembly of spheres. In these examples, the preformed spheres or arrays of spheres direct the mesoscale organization of nanoscale QDs within the photonic crystal, along with providing mesoscale modulation of the refractive index; coupling between nanoparticle emission and photonic pseudogaps has been demonstrated in several of these systems.[1−4,9,11,12] However, current strategies for incorporating nanoparticles into photonic arrays still offer limited control over several additional factors which can influence the collective optical properties of photonic

* To whom correspondence should be addressed. E-mail: mmoffitt@uvic.ca.

† Konkuk University.

(1) Vlasov, Y. A.; Luterova, K.; Pelant, I.; Honerlage, B.; Astratov, V. N. *Appl. Phys. Lett.* **1997**, *71*, 1616.

(2) Blanco, A.; Lopez, C.; Mayoral, R.; Miguez, H.; Meseguer, F.; Mifsud, A.; Herrero, J. *Appl. Phys. Lett.* **1998**, *73*, 1781.

(3) Zhou, J.; Zhou, Y.; Buddhudu, S.; Ng, S. L.; Lam, Y. L.; Kam, C. H. *Appl. Phys. Lett.* **2000**, *76*, 3513.

(4) Gaponeko, S. V.; Bogomolov, V. N.; Petrov, E. P.; Kapitonov, A. M.; Yarotsky, D. A.; Kalosha, I. I.; Eychmueller, A. A.; Rogach, A. L.; McGilp, J.; Woggon, U.; Gindele, F. *J. Lightwave Technol.* **1999**, *17*, 2128.

(5) Vlasov, Y. A.; Yao, N.; Norris, D. J. *Adv. Mater.* **1999**, *11*, 165.

(6) Rogach, A. L.; Nagesha, D.; Ostrander, J. W.; Giersig, M.; Kotov, N. A. *Chem. Mater.* **2000**, *12*, 2676.

(7) Rogach, A. L.; Susha, A.; Caruso, F.; Sukhorukov, G.; Kornowski, A.; Kershaw, S.; Mohwald, H.; Eychmueller, A. A.; Weller, H. *Adv. Mater.* **2000**, *12*, 333.

(8) Zhang, J.; Coombs, N.; Kumacheva, E. *J. Am. Chem. Soc.* **2002**, *124*, 14512.

(9) Wang, D.; Rogach, A. L.; Caruso, F. *Chem. Mater.* **2003**, *15*, 2724.

(10) Yu, A.; Meiser, F.; Cassagneau, T.; Caruso, F. *Nano Lett.* **2004**, *4*, 177.

(11) Lodahl, P.; van Driel, A. F.; Nikolaev, I. S.; Irman, A.; Overgaag, K.; Vanmaekelbergh, D.; Vos, W. L. *Nature* **2004**, *430*, 654.

(12) Zhang, J.-Y.; Wang, X.-Y.; Ye, J.-H.; Xiao, M. *J. Mod. Opt.* **2004**, *51*, 2493.

(13) Yablonovitch, E. *Phys. Rev. Lett.* **1987**, *58*, 2059.

(14) John, S. *Phys. Rev. Lett.* **1987**, *58*, 2486.

(15) Ballato, J.; Dimaio, J.; James, A.; Gulliver, E. *Appl. Phys. Lett.* **1999**, *75*, 1497.

(16) Blanco, A.; Chomski, E.; Grabtchak, S.; Ibisate, M.; John, S.; Leonard, S. W.; Lopez, C.; Meseguer, F.; Miguez, H.; Mondia, J. P.; Ozin, G. A.; Toader, O.; van Driel, H. M. *Nature* **2000**, *405*, 437.

(17) Xia, Y.; Gates, B.; Li, Z.-Y. *Adv. Mater.* **2001**, *13*, 409.

(18) Lopez, C. *Adv. Mater.* **2003**, *15*, 1679.

(19) Wu, H.; Thalladi, V. R.; Whitesides, S.; Whitesides, G. M. *J. Am. Chem. Soc.* **2002**, *124*, 14495.

10.1021/la7002904 CCC: $37.00
Published on Web 04/17/2007

Scheme 1. Hierarchical Self-Assembly Route to Photonic Arrays Containing QDs

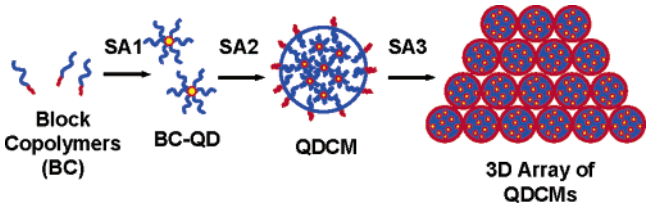

assemblies, including QD−QD interparticle distance and the refractive index at the QD surface.[6] Therefore, a method providing structural control at all functional length scales should open new opportunities for the design of devices.

The three steps of the hierarchical self-assembly strategy utilized here are described in Scheme 1. The first step (SA1) is the self-assembly of an amphiphilic polystyrene-*b*-poly(acrylic acid) (PS-*b*-PAA) block copolymer (BC) in an organic solvent via addition of cadmium acetate, forming reverse micelles with a Cd^{2+}-containing core and a hydrophobic PS corona; within each micelle core, the cadmium ions are then converted to a single cadmium sulfide (CdS) QD to yield nanoscale BC-stabilized QDs (BC−QD). The BC−QD building blocks are kinetically frozen by the high glass transition temperature of the poly(cadmium acrylate) (PACd) layer surrounding each QD, so that the micelles remain intact in the subsequent steps.[20] Once step SA1 is completed, the hydrophobic BC−QD building blocks are blended with amphiphilic PS-*b*-PAA stabilizing chains in a relatively polar organic solvent, dimethylformamide (DMF). Dropwise water addition then induces secondary self-assembly (SA2) via phase separation of the PS blocks, forming mesoscale spherical assemblies of BC−QDs termed quantum dot compound micelles (QDCMs);[21,22] these spheres become frozen due to the glassy nature of the PS blocks when DMF is removed by dialysis. In the final, tertiary self-assembly step (SA3), aqueous dispersions of QDCMs are slowly evaporated to form three-dimensional (3D) arrays of QDCMs with mesoscale periodicity, in some cases resulting in crystalline domains on the micrometer scale.

The final arrays of QDCMs possess a complex structural hierarchy, with nanoscale, mesoscale, and microscale order arising from the sequential self-assembly steps. Organization at each self-assembly step is determined by the experimental conditions (e.g., polymer concentration, speed of water addition) and also by the structures of the building blocks, which are determined by the previous self-assembly step. Therefore, a high degree of structural control is possible at each level of organization by the judicious selection of experimental variables, allowing various parameters governing the collective optical properties, including QD size, nanoparticle spacing, and mesoscale periodicity, to be independently tuned. An additional feature of this strategy is that a constant refractive index is maintained at the QD surface within a stable block copolymer micelle.

Figure 1 shows representative transmission electron microscopy (TEM; parts a and b) and scanning electron microscopy (SEM; part c) images following each step of hierarchical self-assembly; the drawings to the right of each image depict the corresponding organization of the components, with dotted lines circling the main self-assembled elements at the various levels of structural hierarchy. The combination of length scales in the final structure is indicated by a roughly 1 order of magnitude decrease in magnification for structural characterization following each successive step.

The SA1 step was carried out using the block copolymer PS-(300)-*b*-PAA(12) (numbers in brackets indicate number-average degrees of polymerization of each block). Templated synthesis of a cadmium sulfide QD in the core of each BC reverse micelle was carried out by reaction with hydrogen sulfide (H_2S) followed by treatment with cadmium acetate to form a stable PACd layer surrounding each QD. The TEM images of the resulting BC−QD particles (Figure 1a) cast from benzene solution show the dark electron-dense QDs of the individual BC−QD particles. From TEM, the average diameter of the individual CdS QDs is 2.9 nm. From static light scattering of the BC−QDs in DMF solutions, each QD is surrounded by an average of 54 copolymer chains, with an overall particle radius of gyration of $r_g = 21$ nm (including the BC layer).

For the SA2 self-assembly of the BC−QD building blocks, the BC−QDs and the amphiphilic copolymer PS(665)-*b*-PAA-(68) were codissolved in DMF followed by dropwise water addition and subsequent dialysis to remove DMF. As a result of PS phase separation, water-dispersible spherical assemblies (QDCMs) formed, each consisting of multiple assembled BC−QD particles surrounded by a stabilizing layer of the PS(665)-*b*-PAA(68) chains, with the external PAA blocks maintaining colloidal stability in water (Figure 1b). We have recently shown that QDCM particle sizes and polydispersities can be kinetically controlled via the initial polymer concentration in DMF for a constant speed of water addition.[22] QDCM dispersions prepared from an initial polymer concentration of 2.0 wt % (Figure 1b) were imaged by casting the particles from water onto a TEM grid followed by Pt/Pd shadowing; the clustering of spherical particles on the grid is an artifact resulting from water evaporation and does not suggest agglomeration in water. The average core diameter of these particles determined from TEM is $d_{QDCM} = 110$ nm, with a standard deviation (sd) of 17%; this diameter excludes the relatively thin PAA layer, which in water at pH = 6 is determined by dynamic light scattering to be ~17 nm thick. The inset to Figure 1b shows a TEM image of a single QDCM particle without Pt/Pd shadowing, revealing multiple well-dispersed QDs within each secondary assembly. The nearest-neighbor distance between QDs within the QDCMs is determined by the length of the PS coronal chains and the aggregation number of the BC−QD building blocks, which are controllable via the BC composition used in the SA1 step. For the present BC−QD particles, surrounded by an average of 54 PS chains of 300 styrene units each, we have calculated an interparticle distance of 12 nm between the QDs within the mesoscale spheres.[22]

The final self-assembly step (SA3) involved slow water evaporation from the QDCM dispersions on a glass or quartz substrate, such that a combination of capillary and convective forces resulted in the 3D ordering of QDCM spheres in close-packed assemblies. For arrays formed from the QDCM dispersion shown in Figure 1b, the SEM image in part c shows the close packing of spheres with hexagonal crystalline regions within layers (inset) extending, in some cases, over a few microns. The observed extent of 3D ordering is currently limited by the

(20) Wang, C.-W.; Moffitt, M. G. *Langmuir* **2004**, *20*, 11784.
(21) Moffitt, M.; Vali, H.; Eisenberg, A. *Chem. Mater.* **1998**, *10*, 1021.
(22) Yusuf, H.; Kim, W.-G.; Lee, D.-H.; Guo, Y.; Moffitt, M. G. *Langmuir* **2007**, *23*, 868.

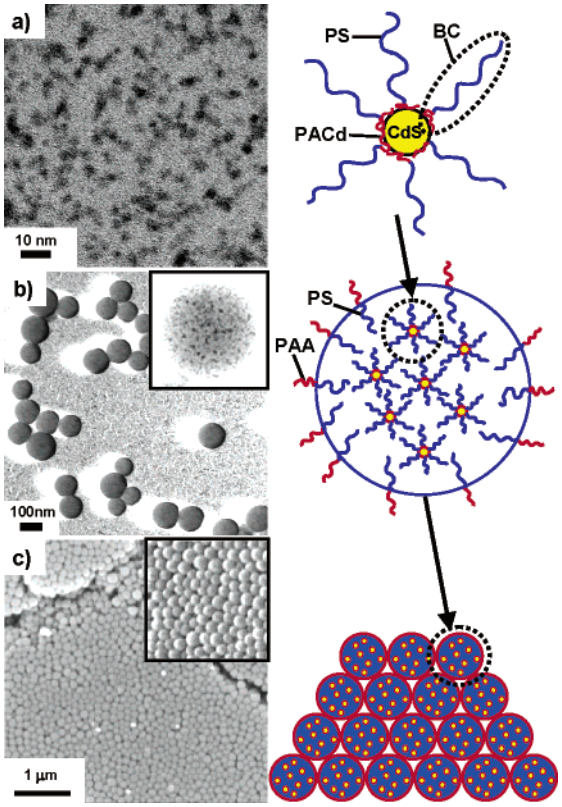

Figure 1. TEM (a,b) and SEM (c) micrographs and accompanying schematics of self-organized structures obtained following each successive self-assembly step: (a) TEM image of BC−QDs formed from the self-assembly of BCs (SA1); (b) TEM image of QDCMs formed from the self-assembly of BC−QDs (SA2); and (c) SEM image of a 3D photonic array formed from the self-assembly of QDCMs (SA3).

polydispersity of the spheres formed via self-assembly (sd = 17%), compared to the ordering of relatively monodisperse silica or polymer spheres formed via synthetic routes; however, we do not believe this to be an inherent limitation of the hierarchical approach, and demonstrated kinetic methods for controlling QDCM polydispersities in the SA2 step are being optimized in our lab.[22] The repulsive interactions between the negatively charged PAA chains on the surfaces of the QDCM particles in water at pH = 6 play a critical role in the ordering of the spheres; when the pH of the same QDCM dispersion was lowered to pH = 4 before drying, the resulting films showed no close-packed or well-ordered regions, due to the apparent sticky interactions between the QDCM spheres.

The hierarchical 3D arrays of QDCMs represent periodic dielectric structures with a modulating refractive index provided by the QDCM spheres and the air voids within the close-packed film. Due to the mesoscale size of the QDCM spheres, such arrays represent potential photonic structures for visible wavelengths. For a 3D array of QDCMs formed using an initial polymer concentration of 2.0 wt % in the SA2 step (Figure 2a), the transmission spectra show a clear stop band in the visible region for various incidence angles with respect to the surface normal (Figure 2b). The stop band does not exhibit a strong angular dependence, which is attributed to the polycrystalline nature of the array combined with a relatively large spot size (∼1 mm) for transmission measurements. From the zero-angle stop band position, λ_{min} = 420 nm, and assuming an effective refractive index, n_{eff} = 1.4, for close-packed QDCM spheres (volume fraction = 74%),[23] we obtain an interplanar spacing of d_{hkl} = 150 nm using the Bragg equation for a first-order reflection: $m\lambda_{min} = 2d_{hkl}(n_{eff}^2 - \sin^2\theta)^{1/2}$. Based on the apparent polycrystallinity of the array, this spacing represents an average distance for a random orientation of crystal planes and is consistent with the hydrodynamic diameter of the QDCM building blocks in water at pH = 6 (d_h = 143 nm).[22] This is very reasonable assuming that a swollen PAA layer surrounding each QDCM contributes to the overall sphere size within the close-packed array.

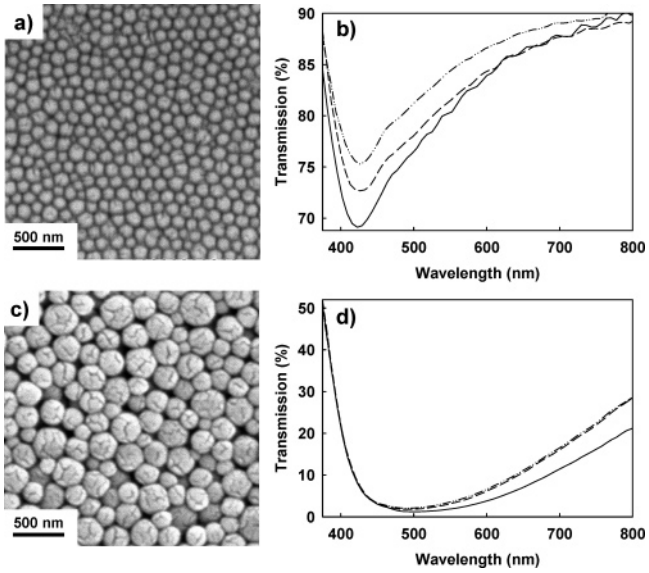

Figure 2. SEM micrographs (a,c) and optical transmission spectra (b,d) for photonic arrays formed by hierarchical self-assembly using different initial polymer concentrations in DMF for the SA2 step: (a,b) 2 wt % and (c,d) 3 wt %. All other conditions for self-assembly are identical. In (c) and (d), the transmission spectra have been obtained for different angles of incidence to the film normal: 20° (− · · −), 40° (- - -), and 60° (—).

The observed stop band is a collective optical property determined by the organization of BC−QDs on the length scale of optical wavelengths. The stop band is therefore tunable via the conditions of either SA2 or SA3 self-assembly. To demonstrate this, we used a different initial polymer concentration for SA2 self-assembly to obtain a second QDCM population, which was then self-assembled into a 3D photonic structure using identical conditions for SA3 self-assembly. For the same BC−QD building blocks, increasing the initial polymer concentration from 2.0 wt % to 3.0 wt % for the SA2 step increased the average QDCM particle size from d_{QDCM} = 109 nm to d_{QDCM} = 209 nm, while the polydispersity increased from 17% to 30%.[22] Compared to the 3D array shown in Figure 2a, the array formed using the larger, more polydisperse QDCMs (Figure 2c) shows a larger average spacing, as well as markedly less order, which is attributed to the increased QDCM polydispersity precluding hexagonal close-packing within the layers: with no discernible crystalline domains, the latter array is therefore best described as a "photonic glass".[15] As a result, the transmission spectrum of the glassy array (Figure 2d) shows an extremely broad minimum at λ_{min} = 490 nm, which is red-shifted compared to the relatively narrow stop band of the polycrystalline array (Figure 2b). As well, the stop band attenuation from the array shown in Figure 2c, with near 0% transmission at 490 nm (Figure 2d), is found to be significantly greater than that from the array shown in Figure 2a, with ∼75% transmission at 420 nm (Figure 2b); this is attributed to a thicker film arising from the vertical deposition of the larger

(23) The volume fraction of QDs within the QDCM sphere is determined to be <1%, so that the spheres are assumed to be effectively PS with n = 1.54.

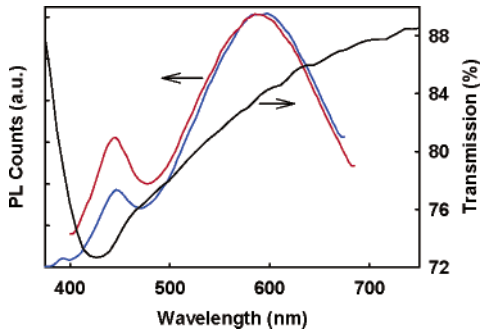

Figure 3. Photoluminescence (red) and transmission (black) spectra of the photonic array shown in Figure 2b. The emission spectrum was obtained with back-face excitation of the film at a 40° detection angle, and the transmission spectrum was obtained using 40° incidence to the surface normal. The blue curve shows the photoluminescence spectrum of BC−QDs dispersed in toluene (without SA2 and SA3 self-assembly) for comparison. For both the solution and the 3D array, an excitation wavelength of $\lambda_{ex} = 350$ nm was used.

QDCM particles. By a simple variation in the conditions of the SA2 step, therefore, the optical properties of the photonic array are tuned.

Along with the collective property of a photonic stop band, these hierarchical arrays show photoluminescence from the constituent CdS QDs formed in the SA1 step. Figure 3 (red curve) shows the emission spectrum from the more ordered of the two photonic arrays, along with the corresponding transmission spectrum; the emission spectrum of the constituent BC−QD particles, dispersed in toluene solution without SA2 self-assembly (blue curve), is shown for comparison. The quantum yields for similar BC−QD particles in toluene have been shown to be in the range of 3−4%, using perylene in ethanol as a reference.[20] The position and shape of the QD emission bands at $\lambda_{em} = 450$ and 600 nm, attributed to near-band edge and surface trap states, respectively, are very similar for the two photoluminescence spectra. This indicates that the size and local surface environment of the QDs remain constant during the SA2 and SA3 self-assembly steps, as the BC−QD cores encapsulate and protect the QD surfaces, while the PS coronal chains ensure good dispersion and control the distances between nanoparticles.

The similarity of the emission spectra before and after the hierarchical self-assembly of BC−QDs also indicates that the periodic dielectric environment of the photonic array does not significantly modify the QD emission. This is likely due to a combination of both the limited attenuation and position of the transmission minimum in Figure 3, which falls below the 450 nm emission peak in a spectral region of low photoluminescence intensity. However, although coupling between QD emission and the stop band is not observed in the present case, the independent control of nanoscale and mesoscale self-assembly demonstrated here should provide routes to narrower and deeper stop bands which can be tuned in the QD emission region. We have shown that the width of the stop band increases significantly with QDCM polydispersities, which are still somewhat high compared to those of mesoscale particles fabricated by synthetic methods such as emulsion polymerization. Various strategies for decreasing QDCM polydispersities at the SA2 step, including fast quenching by increased rates of water addition, should improve long-range order in general while extending the mesoscale periodicies of hierarchical arrays to longer wavelengths. Increased refractive index contrast via the chemical modification of PAA chains at the QDCM surfaces should also provide interesting routes to improving the collective optical properties of the arrays.

In summary, we have demonstrated a three-step hierarchical approach to the formation of photonic arrays containing QDs, in which sequential self-assembly steps introduce organization on progressively longer length scales, ranging from the nanoscale to the microscale regimes. This strategy should provide new opportunities for tuning the properties of QD assemblies for numerous applications in photonics by providing independent control of QD organization on a wide range of disparate functional length scales.

Acknowledgment. This work is supported by the National Science and Engineering Research Council (NSERC), the Canadian Foundation for Innovation (CFI), and the British Columbia Knowledge Development Fund (BCKDF).

Supporting Information Available: Experimental details for the synthesis and characterization of the hierarchical arrays, including a detailed description of the conditions for each of the sequential self-assembly steps. This material is available free of charge via the Internet at http://pubs.acs.org.

LA7002904